

**Metachronal motion of artificial magnetic cilia**

Journal:	<i>Soft Matter</i>
Manuscript ID	SM-COM-03-2018-000549.R1
Article Type:	Communication
Date Submitted by the Author:	19-Apr-2018
Complete List of Authors:	Hanasoge, Srinivas; Georgia Institute of Technology, Woodruff School of Mechanical Engineering Hesketh, Peter; Georgia Institute of Technology, George W. Woodruff School of Mechanical Engineering Alexeev, Alexander; Georgia Institute of Technology, Woodruff School of Mechanical Engineering

1 **Metachronal motion of artificial magnetic cilia**

2 Srinivas Hanasoge, Peter J. Hesketh, Alexander Alexeev
3 George W. Woodruff school of Mechanical Engineering,
4 Georgia Institute of Technology, Atlanta, GA, USA, 30332
5

6 Organisms use hair-like cilia that beat in a metachronal fashion to actively transport fluid and
7 suspended particles. Metachronal motion emerges due to a phase difference between beating
8 cycles of neighboring cilia and appears as traveling waves propagating along ciliary carpet. In
9 this work, we demonstrate biomimetic artificial cilia capable of metachronal motion. The cilia
10 are micromachined magnetic thin filaments attached at one end to a substrate and actuated by a
11 uniform rotating magnetic field. We show that the difference in magnetic cilium length controls
12 the phase of the beating motion. We use this property to induce metachronal waves within a
13 ciliary array and explore the effect of operation parameters on the wave motion. The metachronal
14 motion in our artificial system is shown to depend on the magnetic and elastic properties of the
15 filaments, unlike natural cilia, where metachronal motion arises due to fluid coupling. Our
16 approach enables an easy integration of metachronal magnetic cilia in lab-on-a-chip devices for
17 enhanced fluid and particle manipulations.

18 **Keywords** – Biomimetic artificial cilia, metachronal waves, magnetic cilia.

1 Biological organisms use organelles such as hair-like cilia to perform vital functions
2 involving fluid manipulation in their vicinity. Each cilium performs time-irreversible motion,
3 traversing a spatially asymmetric path, and generates local fluid transport. It is often observed
4 that carpets of natural cilia beat in a metachronal fashion, which appear as propagating waves.
5 For example, lung cilia beat in a metachronal fashion to facilitate the net transport of fluid and
6 microscopic particulates.¹⁻³ Similar metachronal motion is found on larger scales in the gait of
7 millipedes, spiders and other invertebrates.⁴

8 In natural cilia, metachronal motion usually emerges as a self-organized phenomenon due
9 to hydrodynamic coupling between a cilium and its neighbors.^{3,5-7} As a result, tiny flexible cilia
10 beat with a phase difference with respect to their neighbors, thereby generating travelling waves
11 propagating along the ciliary carpet. The direction of metachronal waves in natural cilia can be
12 symplectic (in the direction of the effective stroke), antiplectic (opposite to the direction of
13 effective stroke), or laeoplectic (perpendicular to the direction of effective stroke).⁸

14 Studies point to specific advantages in the use of metachronal motion by natural cilia.^{9,10}
15 It has been reported that such motion can lead to a 3-fold increase in propulsion rate and a 10-
16 fold increase in efficiency compared to synchronously beating cilia.³ Metachronal beating is
17 more energetically efficient and requires a decreased amount of adenosine triphosphate (ATP)
18 consumed by cilia.¹¹ Furthermore, metachronal beating is advantageous in creating a
19 unidirectional fluid pumping.¹² The attractive advantages offered by metachronal beating of
20 natural cilia have motivated researchers to explore artificial analogs of ciliary carpets capable of
21 performing metachronal motion that could be harnessed in microfluidic devices for efficient fluid
22 transport and particle manipulation.^{1-3,6,13,14}

23 To create metachronal motion artificially, it is essential to impose a phase difference in
24 the beating cycles of multiple individual cilia. Such phase difference can be achieved by either
25 applying different forcing to each cilium or by having cilia with different responses to a uniform
26 forcing applied to the entire cilium array. The later approach that relies on a uniform actuation is
27 more attractive from an experimental point of view. Indeed, large arrays of identical artificial
28 cilia¹⁵⁻¹⁹ have been previously actuated by a uniform magnetic force to explore microfluidic
29 applications of their synchronous beating.²⁰⁻²² Only recently a uniform magnetic force was used
30 by Tasumori et al.²³ to demonstrate metachronal motion in an array of artificial magnetic cilia

1 that had a different magnetic orientation. The $2mm$ cilia were created using a sophisticated
 2 fabrication method that required carefully monitored processing steps with each cilium
 3 fabricated individually. The authors intend to miniaturize their cilia to a sub-millimeter size in
 4 the future work.

5 In this work, we explore a new approach to create metachronal motion in an array of
 6 magnetic cilia submerged in a viscous fluid and actuated by a uniform rotating magnetic field.
 7 High-aspect-ratio magnetic filaments that are periodically deformed by a rotating magnetic field
 8 have been previously suggested as an attractive approach to create artificial beating cilia.²⁴ We
 9 use cilia that are made up of paramagnetic metallic filaments with identical magnetic
 10 properties.^{25,26} The motion of such cilia in a rotating magnetic field is defined by magnetic,
 11 elastic, and viscous hydrodynamic forces. The counter-clockwise rotating magnetic field bends
 12 the elastic cilium during the forward stroke, during which elastic energy is accumulated. After
 13 reaching maximum bending, cilia recover to the initial position by releasing the accumulated
 14 elastic energy. At relatively low actuation frequencies, the forward stroke is governed by a
 15 balance of the magnetic and elastic forces, whereas the recovery stroke is controlled by an
 16 interplay of the elastic and viscous forces.¹⁹

17 Metachronal wave motion in a ciliary array emerges when there is a phase difference in
 18 beating strokes of neighboring cilia, such that neighboring cilia transition from the forward to the
 19 recovery stroke in a sequential manner. In our system, the transition happens when the elastic
 20 force in deformed cilia exceeds the magnetic force due to the rotating magnet. More flexible cilia
 21 deflect more easily by the magnetic field²⁴ and, therefore, transition to the recovery at larger
 22 rotational angles of the magnet compared to stiffer cilia with the same magnetic properties. This
 23 leads to a phase difference between the beating of more flexible and less flexible magnetic cilia.
 24 In this work, we harness this property to fabricate an array of cilia that exhibit metachronal
 25 motion under uniform rotating magnetic field.

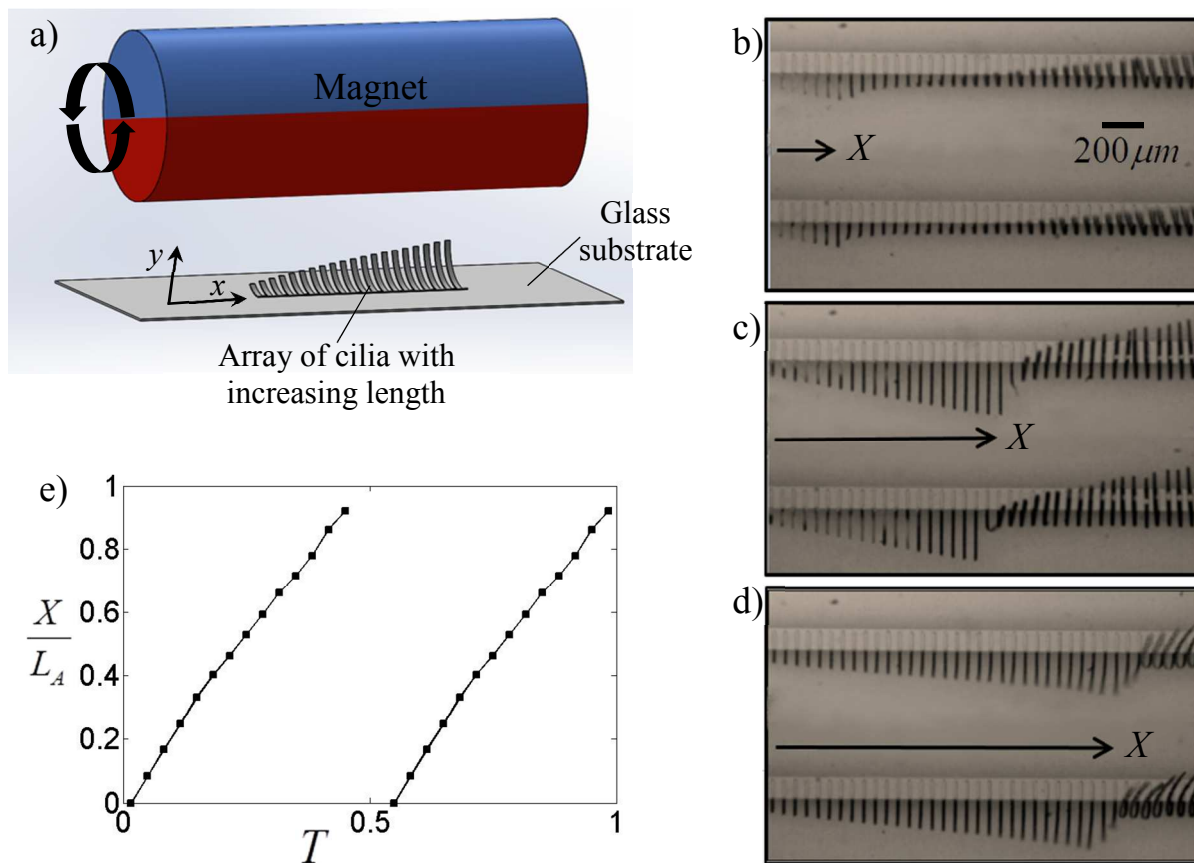
26 We consider elastic cilia that are made of a paramagnetic material. In this case, the ratio
 27 between magnetic and elastic forces acting on a cilium can be characterized by a magnetic
 28 number $Mn = BL(WP/\mu_0 EI)^{0.5}$. Here, $B = |\mathbf{B}|$ is the magnitude of the externally-applied
 29 magnetic flux density, $\mu_0 = 4\pi \times 10^{-7}$ is the permeability of free space, E is the Yung's modulus,

1 $I = WP^3/12$ is the bending moment of inertia, and L , W , P are the length, width, and thickness
 2 of the cilium, respectively.^{25,27–29} Note that in the above definition of Mn , W cancels out and,
 3 therefore, Mn is independent of cilium width. Note also that a similarly defined magnetoelastic
 4 number has been previously successfully employed in numerical simulations to describe
 5 kinematics of magnetic cilia.^{24,30,31}

6 To achieve metachronal motion, we can change the magnet angle at which cilia transition
 7 from forward to recovery stroke and, therefore, the phase of cilium beating, by altering the
 8 magnitude of Mn for individual filaments in a ciliary array. Since Mn linearly depends on the
 9 cilium length L , a linear change of cilium length should lead to a metachronal wave propagating
 10 along the ciliary array with a constant speed. To test this hypothesis, we fabricated a cilium array
 11 with cilium length increasing linearly with the cilium position along the array.

12 An array of nickel iron permalloy cilia is fabricated using surface micromachining with
 13 cilium length increasing from $60\mu\text{m}$ to $600\mu\text{m}$. The cilia are $10\mu\text{m}$ in width, and 60nm in
 14 thickness. The separation between neighboring cilia within a row is $50\mu\text{m}$, unless indicated
 15 otherwise. Multiple rows of cilia with separation 1mm are firmly attached to a glass slide and
 16 visualized using an inverted microscope (Nikon Eclipse Ti). Details of the fabrication process
 17 and imaging procedure can be found elsewhere.²⁵ The cilia are actuated by a permanent magnet
 18 with a 12mm diameter rotating with a constant frequency f . The large size of the magnet
 19 compared to the ciliary array ensures a uniform magnetic field experienced by cilia. A schematic
 20 of the experimental setup is shown in Fig. 1a.

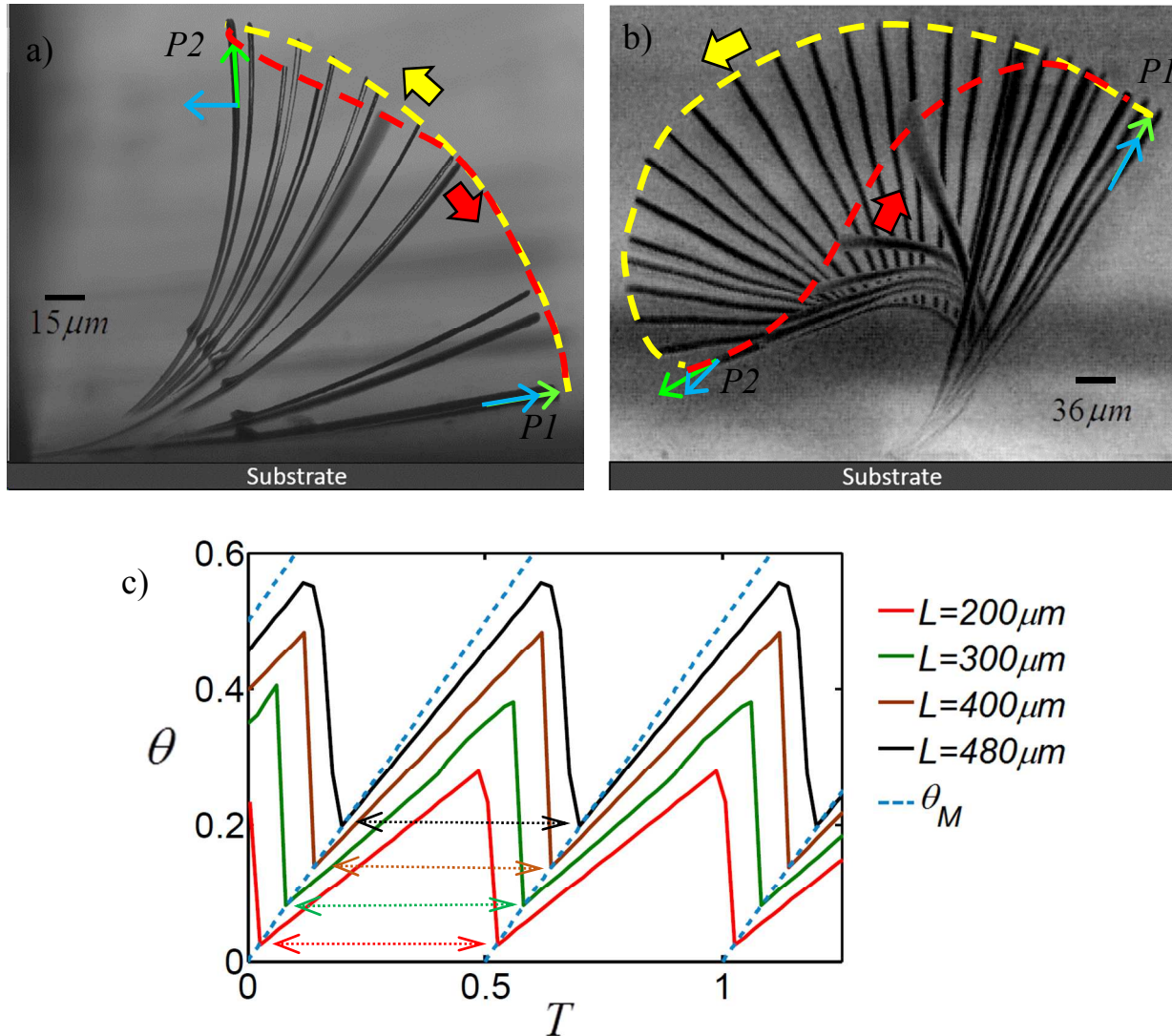
21 Figures 1b, 1c, and 1d show snapshots of the ciliary array at different times during the
 22 magnet rotation. The snapshots illustrate the propagation of a metachronal wave along the array
 23 (also see Video 1 in ESI). We identify the front of the metachronal wave by the position of the
 24 cilia within the array that have just completed the recovery stroke, as indicated by the arrows in
 25 Figs. 1b, 1c, and 1d. We find that the metachronal wave propagates from the shorter cilia on the
 26 left to the longer cilia on the right with a nearly constant speed. This is indicated by the linearly
 27 increasing position of the wave front with time T (Fig. 1e). Note that front position X is
 28 normalized by total length of the array L_A . In our current implementation, the metachronal
 29 motion is perpendicular to the direction of the effective cilium stroke (i.e., laeoplectic).



1
 2 **Figure 1. a)** Schematic of the experimental setup with an array of cilia with linearly varying
 3 lengths actuated by a permanent magnet rotating. **b-d)** Snapshots of the ciliary array at time
 4 $T = 0.1$, $T = 0.25$, and $T = 0.45$, respectively. Two rows of cilia are shown. The magnet is
 5 rotated counter clockwise with a frequency of $0.5Hz$. Metachronal motion can be viewed from
 6 left to right from below the glass substrate, with the wave front indicated by the arrow. See ESI
 7 for videos of metachronal wave motion in ciliary arrays. **e)** Position of the metachronal wave
 8 front $\chi = X/L_A$, where L_A is the array length, as a function of time T . Time T is normalized by
 9 the period of magnet rotation.

10

11 To further understand how the metachronal beating is created in our ciliary array, we
 12 examine the kinematics of two beating cilia with different length. Figures 2a and 2b present a
 13 series of overlapped images of cilia with length $L = 220\mu m$ and $L = 480\mu m$, respectively. In
 14 both cases, cilium tips follow closed trajectories shown by a yellow line during the forward
 15 stroke and by a red line during the recovery stroke.



1
 2 **Figure 2.** Motion of a single cilium in a beating cycle with length **a)** $L = 200\mu\text{m}$ and **b)**
 3 $L = 480\mu\text{m}$. The yellow and red arrows indicate the forward and recovery strokes, respectively.
 4 The green arrow is tangent to the cilium tip and the blue arrow indicates the direction of the
 5 magnetic field. **c)** The tip angle of beating cilia as a function of time T . The dotted lines show
 6 the rotational angle of the magnetic field. The angles are measured with respect to the substrate
 7 and are normalized by 2π . Time is normalized by the period of the external magnetic field
 8 rotation equal to $2s$.

9 The forward stroke starts at position $P1$. For both the cilia, the tip angle, indicated by the
 10 green arrow, is closely aligned with the direction of the magnetic field, indicated by the blue
 11 arrow. The CCW rotating field induces a magnetic moment that bends the cilia in the counter-
 12 clockwise direction. The cilium tip angle increases and reaches a maximum at position $P2$. At

1 this position of the maximum bending, the elastic force due to cilium deformation exceeds the
 2 magnetic force causing the beginning of the recovery stroke. Position $P2$ is determined by the
 3 value of Mn . Shorter cilia with larger stiffness, and therefore a lower Mn , bend to a lesser
 4 extent (Fig. 2a), whereas longer cilia with lower stiffness and higher Mn are capable of bending
 5 to larger angles to follow the field (Fig. 2b). Thus, the maximum bending angle at position $P2$ is
 6 greater for the longer cilia that are characterized by higher values of Mn .

7 At position $P2$, the angle between the cilium tip and magnetic field is larger for the
 8 shorter cilium compared to the longer cilium, as indicated by the angle between the red and blue
 9 arrows in Fig. 2. Further rotation of the magnet beyond $P2$ reduces the magnetic moment and
 10 the cilia return to position $P1$ releasing the accumulated elastic energy. The shorter cilium
 11 returns to $P1$ at a smaller magnet angle than the longer cilium leading to a phase difference in
 12 the beating cycle that is proportional to the cilium length. Note that magnetization of the cilia
 13 flips its direction during the recovery stroke. As a result, cilia perform two beating cycles for
 14 each rotation of the magnetic field.^{25,27,32}

15 The phase offset in the motion of different length cilia is illustrated in Fig. 2c. Here, we
 16 plot the normalized tip angle θ as a function of time T . Tip angle θ is measured with respect to
 17 the substrate in the counter-clockwise direction. Time T is normalized by period of the magnetic
 18 field. The increasing value of θ indicates the forward stroke, whereas the decreasing θ
 19 represents the recovery stroke. The angle of the magnetic field θ_M is indicated by the tilted
 20 dotted lines.

21 The forward stroke starts when the direction of the magnetic field θ_M coincides with the
 22 tip angle θ . This happens at different T for cilia with different length, with shorter cilia
 23 initiating the forward stroke earlier than longer cilia. The tip angle increases nearly linearly with
 24 T until the maximum is reached. As cilia deform, the difference between the cilia tip angle θ
 25 and the direction of magnetic fields θ_M increases, indicating the lag in cilium tip angle with
 26 respect to the magnet. This difference is larger for shorter cilia which are effectively stiffer. The
 27 maximum θ coincides the beginning of the recovery stroke, which starts earlier for shorter cilia.
 28 During the recovery stroke, θ decreases until it matches the direction of the magnetic field and
 29 then the cycle repeats. Thus, cilia of different length perform cyclic motion with period matching

1 the half period of the magnet rotation, but with different phases with respect to the rotation of the
 2 magnetic field. The phase is proportional to the effective bending elasticity of the cilia and, thus,
 3 depends on the magnitude of the magnetic number Mn . Remember, $Mn = BL(WP/\mu_0 EI)^{0.5}$
 4 represents the ratio between the magnetic force that is constant in our experiments and the elastic
 5 forces that is proportional to the cilium length. As a result, a metachronal wave emerges that
 6 propagates in the direction of the increasing cilium length (see Video 2 in ESI that shows two
 7 metachronal waves simultaneously propagating in opposing directions within a ciliary array with
 8 different cilium lengths).

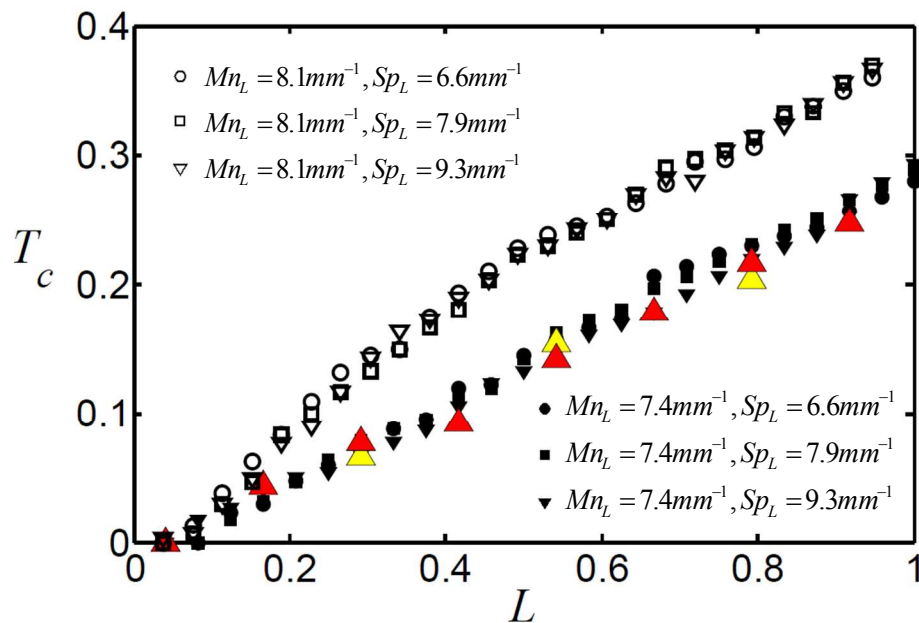
9 In addition to the magnetic number Mn , cilium beating is characterized by the Reynolds
 10 number $Re = \rho LWf/\mu$ and the sperm number $Sp = L(\omega\xi/EI)^{0.25}$.^{25,29,32} Here, ρ is the fluid
 11 density, $\omega = 2\pi f$ is the cilium angular velocity, and $\xi = 4\pi\mu$ is the lateral drag coefficient of
 12 the cilium with μ being the fluid dynamic viscosity. The Reynolds number represents the
 13 importance of inertial hydrodynamic forces. In our experiments, the longest cilium length is
 14 $L = 600\mu m$ and the fastest actuation frequency is $f = 4Hz$, leading to the maximum $Re = 0.02$,
 15 indicating that fluid inertia has a negligible effect on cilium motion.

16 The sperm number Sp characterizes the ratio of viscous to elastic forces acting on cilia.
 17 To further explore the effect of Sp and Mn on metachronal waves, we conducted experiments
 18 in which we varied both these dimensionless parameters in the ranges from 0 to 6.5 and from 0
 19 to 4.9, respectively. Since, Sp and Mn are both proportional to L , their magnitudes change
 20 along our ciliary arrays. We, therefore, introduce dimensional parameters $Sp_L = Sp/L$ and
 21 $Mn_L = Mn/L$ to describes the operating condition for the entire array. In the experiments, we
 22 vary Sp_L by changing the magnet frequency, whereas Mn_L is changed by altering the distance
 23 from the array to the magnet. Note that Sp_L and Mn_L have the unit of m^{-1} .

24 To characterize the metachronal motion, we measure the time T_c at which a cilium
 25 returns to PI completing a beating cycle (see Fig. 2). In Fig. 3, we plot T_c as a function of the
 26 normalized cilium position $\chi = X/L_A$, where X is the cilium position within the array and

1 $L_A = 3\text{mm}$ is the length of the array. The results are presented for selected values of Sp_L and
 2 Mn_L . Figure 3 shows that T_c increases nearly linearly with χ along the array indicating the
 3 propagation of a metachronal wave with a constant speed. Furthermore, the inverse of T_c slope
 4 represents the wave speed.

5 We find in Fig. 3 that all the data for T_c collapses into two curves corresponding to the
 6 two values of Mn_L tested in our experiments. The results are independent of Sp_L confirming that
 7 the metachronal wave motion is solely defined by Mn_L that sets the speed of the wave
 8 propagation. A lower value of Mn_L results in a faster wave speed. Indeed, weaker magnetic field
 9 can deform cilia to a smaller angle triggering an earlier transition to the recovery stroke.
 10 Therefore, T_c decreases with decreasing Mn_L .



11
 12 **Figure 3.** Cycle completion time T_c as a function of cilium position χ for various experimental
 13 conditions. Note that data points collapse onto separate curves depending on Mn_L , indicating the
 14 weak dependence on Sp_L . The symbols \blacktriangle and \blacktriangleleft represent data obtained for $Mn_L = 7.4\text{mm}^{-1}$,
 15 $Sp_L = 6.6\text{mm}^{-1}$ from arrays with $150\mu\text{m}$ and $300\mu\text{m}$ spacing between cilia, respectively.

16

1 In naturally occurring cilia, metachronal motion emerges as a result of hydrodynamic
2 coupling between neighboring cilia.^{3,5-7} To probe the effect of hydrodynamic interactions
3 between neighboring cilia in our synthetic system, we conducted experiments with ciliary arrays
4 having different distances between cilia within a row. Specifically, we fabricated arrays of cilia
5 with 3 and 6 times greater spacing between the neighboring filaments as compared to our
6 original arrays. The results for T_c obtained in these experiments are indicated in Fig. 3 by the
7 colored symbols. We find that spacing between cilia does not affect metachronal wave
8 propagation. Thus, in our artificial ciliary system the metachronal motion is solely controlled by
9 the interplay between magnetic and elastic forces, and not due to hydrodynamics coupling.

10 In our experimental system, the metachronal wave propagates in the direction
11 perpendicular to cilium beating plane, resulting in laeoplectic metachronal motion. Such
12 laeoplectic metachronal motion has been shown to produce secondary flows with a net fluid flux
13 perpendicular to the beating plane.³³ We note that by changing the spatial arrangement of cilia on
14 the substrate such that cilia with different Mn are placed in front or behind of each other, either
15 symplectic or antiplectic motion can be achieved. It has been shown that for antiplectic
16 metachrony, the net flow generated by cilia is greater, whereas symplectic metachronal beating
17 leads to a flow that is slower in comparison to synchronously beating cilia.³³ Studying the fluid
18 flow produced by magnetic cilia arranged in these different spatial configurations that lead to
19 different cases of metachrony is an important direction of the future investigation that will also
20 enable better understanding of the function of natural cilia.

21 In conclusion, we have demonstrated a new approach to create metachronal waves in an
22 array of artificial cilia submerged in a viscous fluid and actuated by a uniform rotating magnetic
23 field. We use arrays of metallic thin film cilia with varying length and make use of a phase
24 difference in their motion to create periodical traveling waves propagating along the ciliary
25 arrays in the direction of cilium length gradient. We show that the phase of a cilium beating is
26 fully defined by the magnitude of the magnetic number that relates the strength of the magnetic
27 force acting on cilia and cilium elasticity. For a given magnetic flux density, the magnetic
28 number is proportional to cilium length, enabling the use of cilium geometry to induce
29 metachronal motion. We show that this metachronal motion is insensitive to the magnitude of the
30 viscous forces acting on beating cilia and hydrodynamic interactions between neighboring cilia.

1 We note that the magnetic number depends on cilium thickness, but is independent of the cilium
2 width. Thus, we expect that arrays of cilia with identical length and a gradient in cilium thickness
3 will yield a similar metachronal behavior. More generally, metachronal waves can be expected in
4 ciliary arrays with gradients of the magnetic number actuated by a uniform magnetic field.
5 Finally, we note that our fabrication approach enables creation of large arrays of microscopic
6 magnetic cilia that can be readily integrated into various microfluidic devices. This in turn will
7 facilitate the development of attractive biomimetic platforms that use metachronal cilium motion
8 for fluid and particle manipulation.

9 **Acknowledgments**

10 We thank the USDA NIFA (grant #11317911) and the National Science Foundation
11 (CBET-1510884) for financial support and the staff of Georgia Tech IEN for assistance with
12 clean room fabrication.

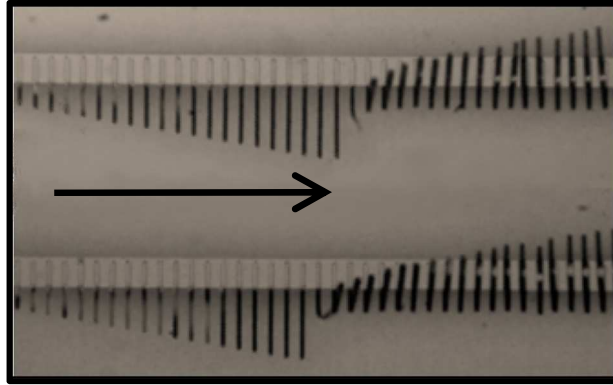
1 **References:**

- 2 1. Blake, J. On the movement of mucus in the lung. *J. Biomech.* **8**, 179–190 (1975).
- 3 2. Mitran, S. M. Metachronal wave formation in a model of pulmonary cilia. *Comput. Struct.* **85**,
- 4 763–774 (2007).
- 5 3. Elgeti, J. & Gompper, G. Emergence of metachronal waves in cilia arrays. *Proc. Natl. Acad.*
- 6 *Sci.* **110**, 4470–4475 (2013).
- 7 4. Wilkinson, M. *The Story of Life in Ten Movements*. (Basic Books, 2016).
- 8 5. Aiello, E. & Sleight, M. A. The metachronal wave of lateral cilia of *Mytilus edulis*. *J. Cell*
- 9 *Biol.* **54**, 493–506 (1972).
- 10 6. Gueron, S., Levit-Gurevich, K., Liron, N. & Blum, J. J. Cilia internal mechanism and
- 11 metachronal coordination as the result of hydrodynamical coupling. *Proc. Natl. Acad. Sci.* **94**,
- 12 6001–6006 (1997).
- 13 7. Sleight, M. A. Coordination of the Rhythm of Beat in Some Ciliary Systems. in *International*
- 14 *Review of Cytology* (eds. Bourne, G. H., Danielli, J. F. & Jeon, K. W.) **25**, 31–54 (Academic
- 15 Press, 1969).
- 16 8. Machemer, H. Ciliary activity and the origin of metachrony in *Paramecium*: effects of
- 17 increased viscosity. *J. Exp. Biol.* **57**, 239–259 (1972).
- 18 9. Osterman, N. & Vilfan, A. Finding the ciliary beating pattern with optimal efficiency. *Proc.*
- 19 *Natl. Acad. Sci.* **108**, 15727–15732 (2011).
- 20 10. Khaderi, S. N., den Toonder, J. M. J. & Onck, P. R. Fluid flow due to collective non-
- 21 reciprocal motion of symmetrically-beating artificial cilia. *Biomicrofluidics* **6**, 014106-
- 22 014106-14 (2012).

- 1 11. Guirao, B. & Joanny, J.-F. Spontaneous Creation of Macroscopic Flow and Metachronal
2 Waves in an Array of Cilia. *Biophys. J.* **92**, 1900–1917 (2007).
- 3 12. Khaderi, S. N., Toonder, J. M. J. den & Onck, P. R. Microfluidic propulsion by the
4 metachronal beating of magnetic artificial cilia: a numerical analysis. *J. Fluid Mech.* **688**, 44–
5 65 (2011).
- 6 13. Masoud, H. & Alexeev, A. Harnessing synthetic cilia to regulate motion of
7 microparticles. *Soft Matter* **7**, 8702–8708 (2011).
- 8 14. Ding, Y. & Kanso, E. Selective particle capture by asynchronously beating cilia. *Phys.*
9 *Fluids* **27**, 121902 (2015).
- 10 15. Fahrni, F., Prins, M. W. J. & van Ijzendoorn, L. J. Micro-fluidic actuation using magnetic
11 artificial cilia. *Lab. Chip* **9**, 3413 (2009).
- 12 16. Vilfan, M. *et al.* Self-assembled artificial cilia. *Proc. Natl. Acad. Sci.* **107**, 1844–1847
13 (2010).
- 14 17. Wang, Y., den Toonder, J., Cardinaels, R. & Anderson, P. A continuous roll-pulling
15 approach for the fabrication of magnetic artificial cilia with microfluidic pumping capability.
16 *Lab. Chip* **16**, 2277–2286 (2016).
- 17 18. Toonder, J. den *et al.* Artificial cilia for active micro-fluidic mixing. *Lab. Chip* **8**, 533
18 (2008).
- 19 19. Hanasoge, S., Hesketh, P. J. & Alexeev, A. Microfluidic pumping using artificial
20 magnetic cilia. *Microsyst. Nanoeng. Press* (2018).
- 21 20. Alexeev, A., Yeomans, J. M. & Balazs, A. C. Designing Synthetic, Pumping Cilia That
22 Switch the Flow Direction in Microchannels. *Langmuir* **24**, 12102–12106 (2008).

- 1 21. Ghosh, R., Buxton, G. A., Usta, O. B., Balazs, A. C. & Alexeev, A. Designing
2 Oscillating Cilia That Capture or Release Microscopic Particles. *Langmuir* **26**, 2963–2968
3 (2010).
- 4 22. Mills, Z. G., Aziz, B. & Alexeev, A. Beating synthetic cilia enhance heat transport in
5 microfluidic channels. *Soft Matter* **8**, 11508–11513 (2012).
- 6 23. Tsumori, F. *et al.* Metachronal wave of artificial cilia array actuated by applied magnetic
7 field. *Jpn. J. Appl. Phys.* **55**, 06GP19 (2016).
- 8 24. Cebers, A. & Livanovics, R. Flexible ferromagnetic filaments as artificial cilia. *Int. J.*
9 *Mod. Phys. B* **25**, 935–941 (2011).
- 10 25. Hanasoge, S., Ballard, M., J. Hesketh, P. & Alexeev, A. Asymmetric motion of
11 magnetically actuated artificial cilia. *Lab. Chip* **17**, 3138–3145 (2017).
- 12 26. Hanasoge, S. *et al.* Active fluid mixing with magnetic microactuators for capture of
13 Salmonella. in (eds. Kim, M. S., Chao, K. & Chin, B. A.) 986405 (2016).
14 doi:10.1117/12.2225571
- 15 27. Khaderi, S. N. *et al.* Nature-inspired microfluidic propulsion using magnetic actuation.
16 *Phys. Rev. E* **79**, 046304 (2009).
- 17 28. Roper, M. *et al.* On the dynamics of magnetically driven elastic filaments. *J. Fluid Mech.*
18 **554**, 167 (2006).
- 19 29. Dreyfus, R. *et al.* Microscopic artificial swimmers. *Nature* **437**, 862–865 (2005).
- 20 30. Goyeau, L., Livanovičs, R. & Cēbers, A. Dynamics of a flexible ferromagnetic filament
21 in a rotating magnetic field. *Phys. Rev. E* **96**, 062612 (2017).
- 22 31. Cebers, A. & Erglis, K. Flexible Magnetic Filaments and their Applications. *Adv. Funct.*
23 *Mater.* **26**, 3783–3795 (2016).

- 1 32. Khaderi, S. N., den Toonder, J. M. J. & Onck, P. R. Magnetically Actuated Artificial
2 Cilia: The Effect of Fluid Inertia. *Langmuir* **28**, 7921–7937 (2012).
- 3 33. Khaderi, S. N. & Onck, P. R. Fluid–structure interaction of three-dimensional magnetic
4 artificial cilia. *J. Fluid Mech.* **708**, 303–328 (2012).
- 5



Bio-mimetic metachronal motion can be created in arrays of artificial magnetic cilia actuated by a rotating magnetic field.